Original Article
Predictive value of CT radiomics and inflammatory markers for pulmonary adenocarcinoma spread through air spaces

Changlei Lv, Guoping Zhang, Bingqiang Xu, Minggang Huang, Yan Zhang, Mingqing Kou

Department of Radiology, Shaanxi Provincial People's Hospital, Xi'an 710068, Shaanxi, China

Abstract: Objectives: To evaluate the predictive value of combining CT radiomics features and inflammatory markers for the preoperative prediction of spread through air spaces (STAS) in pulmonary adenocarcinoma. Methods: In this retrospective study, we analyzed data from 256 patients diagnosed with pulmonary adenocarcinoma between 2021 and 2023. Patients were categorized into two groups based on the presence (n = 115) or absence (n = 141) of STAS, as confirmed by histopathological examination. CT imaging data and routine blood test results, including inflammatory markers, were collected. A validation cohort of 233 patients was included for external validation. Statistical analyses, including univariate and multivariate logistic regression, were performed to identify independent predictors of STAS. Model performance was assessed using Receiver Operating Characteristic curve analysis. Results: Key CT radiomics features, such as density, satellite lesions, irregular shape, spiculation, vascular convergence, and the vacuole sign, were significantly associated with STAS. Among inflammatory markers, a lower lymphocyte-to-monocyte ratio (LMR) and higher neutrophil-to-lymphocyte (NLR) and platelet-to-lymphocyte ratios (PLR) were predictive of STAS. The combined predictive model, integrating CT radiomics and inflammatory markers, demonstrated a high discriminatory ability, achieving an area under the curve of 0.915, which was externally validated with an AUC of 0.847. Conclusions: The combination of CT radiomics and inflammatory markers provides an effective, non-invasive preoperative tool for predicting STAS in pulmonary adenocarcinoma, aiding in early prognostication and treatment planning.

Keywords: Pulmonary adenocarcinoma, spread through air spaces, CT radiomics, inflammatory markers, prognostic model, non-invasive prediction

Introduction

Pulmonary adenocarcinoma is the most prevalent subtype of non-small cell lung cancer (NSCLC), accounting for approximately 40% of all lung cancer cases worldwide [1]. Despite advances in early detection and treatment, it remains a major cause of cancer-related mortality [2]. A critical factor contributing to poor prognosis in pulmonary adenocarcinoma patients is the occurrence of spread through air spaces (STAS), a pattern of tumor invasion that leads to high recurrence rates, reduced overall survival, and challenges in surgical management [3, 4]. Therefore, early and accurate prediction of STAS is crucial for optimizing treatment strategies and improving patient outcomes.

Currently, STAS diagnosis largely relies on histopathological examination following surgical resection, limiting the ability for preoperative risk stratification and personalized treatment planning [5, 6]. This highlights the need for non-invasive predictive tools that can detect STAS before surgery. Radiomics, a field that extracts high-dimensional quantitative features from radiological images using advanced computational techniques, has emerged as a promising solution [7, 8]. Radiomics enables the characterization of tumor heterogeneity and underlying pathophysiological features that may not be visible on conventional imaging, thereby improving diagnostic accuracy and prognostication [9]. Specifically, CT radiomics has shown potential in assessing tumor phenotypes, predicting

treatment responses, and estimating survival outcomes in various cancers, including lung adenocarcinoma [10].

In parallel, the role of systemic inflammation in cancer progression and metastasis has received growing attention [11]. Inflammatory markers, easily obtained from routine blood tests, reflect the interaction between the host immune response and the tumor microenvironment. The lymphocyte-to-monocyte ratio (LMR), which reflects the balance between anti-inflammatory lymphocytes and pro-inflammatory monocytes, has been associated with poorer prognosis in several cancers, including lung adenocarcinoma. A lower LMR indicates a compromised immune environment that may facilitate tumor progression and metastasis [12]. The neutrophil-to-lymphocyte ratio (NLR) is another commonly used marker, where elevated NLR values suggest chronic inflammation, contributing to worse outcomes in lung cancer patients [13]. The platelet-to-lymphocyte ratio (PLR), which assesses the interaction between platelets and lymphocytes, has been linked to poor prognosis in various cancers, including lung adenocarcinoma. Platelets promote tumor growth by releasing growth factors and aiding angiogenesis, while also facilitating tumor cell dissemination through thrombus formation [14]. The Advanced Lung Cancer Inflammation Index (ALI), an important prognostic indicator, evaluates systemic inflammation in lung cancer patients and has predictive value for advanced-stage disease [15]. The Prognostic Nutritional Index (PNI), which combines serum albumin and total lymphocyte count, is widely used to assess nutritional status and surgical risk. Lower PNI values have been associated with poorer outcomes due to compromised immune and nutritional status [16]. The Systemic Immune-Inflammation Index (SII), calculated from platelet, neutrophil, and lymphocyte counts, provides a comprehensive assessment of systemic inflammation and has been linked to worse prognosis in lung cancer [17]. By selecting these markers, we aim to capture different aspects of the host's immune and inflammatory responses to develop a robust predictive model for STAS in pulmonary adenocarcinoma.

This study aims to integrate CT radiomics with inflammatory markers to construct a predictive model for STAS in pulmonary adenocarcinoma.

By combining imaging phenotypes and systemic biomarkers, we seek to develop a non-invasive, cost-effective method for assessing STAS risk and guiding clinical decision-making.

Materials and methods

Ethics statement

This study was approved by the Medical Ethics Committee of Shaanxi Provincial People's Hospital.

Study design

The retrospective study included 256 patients diagnosed with pulmonary adenocarcinoma who were hospitalized at Shaanxi Provincial People's Hospital between 2021 and 2023. Medical records were reviewed to assess the predictive value of CT radiomics and inflammatory markers for STAS in pulmonary adenocarcinoma. Based on histopathological examinations, patients were divided into two groups: those with STAS (STAS group, n = 115) and those without (N-STAS group, n = 141). For external validation, 233 patients with pulmonary adenocarcinoma from another hospital were included, adhering to the same inclusion criteria and grouping standards. In this validation cohort, the STAS group comprised 112 patients and the N-STAS group consisted of 121 patients.

Eligibility and grouping criteria

Inclusion Criteria: The study included patients who met all of the following criteria: (1) Aged 18 years or older. (2) Diagnosed with pulmonary adenocarcinoma based on imaging and molecular biological testing, and subsequently underwent surgical resection of the primary tumor. (3) Tumors classified as T1 or T2 stage according to the 8th edition of the tumor-node-metastasis (TNM) staging system [18]. (4) Chest CT scans with thin sections (≤ 1.5 mm) without artifacts, conducted within one week prior to surgery. (5) Complete CT images that were fully readable by the PACS system and 3D Slicer software. (6) Well-preserved pathological specimens suitable for STAS assessment.

Exclusion Criteria: Patients were excluded if they met any of the following criteria: (1) Poor

image quality. (2) Metastatic pulmonary adenocarcinoma. (3) Specific variants of pulmonary adenocarcinoma. (4) History of neoadjuvant therapy or chemotherapy prior to surgery. (5) Previous history of lung surgery. (6) Incomplete preservation of pathological reports or clinical data. (7) Absence of normal lung margin (at least 1 cm thick) surrounding the entire tumor. (8) Modes of metastasis other than STAS.

CT image collection and segmentation

Before surgery, all enrolled patients underwent contrast-enhanced thin-section CT scans using spiral CT scanners (Siemens SOMATOM Definition Flash and Siemens SOMATOM Force). The scan parameters included a detector collimation width of 64 × 0.6 mm and a tube voltage of 120 kVp, with the tube current automatically adjusted. Images were reconstructed with a slice thickness and gap of 1.5 mm or a slice thickness of 1.5 mm and a gap of 1.0 mm. The reconstruction matrix was set to 512 × 512 pixels. Digital Imaging and Communications in Medicine (DICOM) images were retrieved from the Picture Archiving and Communication System (PACS) and imported into the open-source 3D Slicer software (version 4.11) for analysis.

Two experienced radiologists independently evaluated all CT images using 3D Slicer software to assess the radiological characteristics of the tumors. They manually segmented the regions of interest (ROI) on each CT slice. Both radiologists were blinded to the pathological type and STAS status.

Histopathological evaluation

Following surgery and with the patient's consent, resected tumor tissue was preserved in formalin. Multiple tissue samples were collected from both the tumor and the surrounding lung parenchyma after fixation. Histological sections were prepared from each paraffin block and stained with hematoxylin and eosin for examination under light microscopy. The morphological features of STAS were classified according to the 2021 World Health Organization classification [19], and STAS was further classified based on the extent of circumferential spread. All slides were independently evaluated by two experienced pathologists, and discrepancies were resolved through discussion until a consensus was reached.

*Collection of inflammatory markers*

A nurse collected 4 mL of venous blood from each patient for analysis using an automated hematology analyzer (JS JASON DH-600, Shanghai, China). The analysis included various blood parameters such as serum albumin (ALB), and the absolute counts of neutrophils, lymphocytes, monocytes, and platelets. Inflammatory markers, including the NLR, LMR, and PLR were also calculated. Other indices included the albumin-to-lymphocyte index (ALI), calculated as ALI = body mass index (BMI) × ALB/NLR, the Prognostic Nutritional Index (PNI), calculated as PNI = ALB + 5 × lymphocyte count, and the Systemic Immune-Inflammation Index (SII), expressed as SII = platelet count × NLR. These markers were used to evaluate the patient's level of systemic inflammatory response.

Statistical analysis

Using G*Power 3.1.9.7, a "Means: Difference between two independent means (two groups)" test was selected with a post hoc analysis. The settings were as follows: two-tailed mode, effect size d = 0.5, α err prob = 0.05. The sample sizes for the two groups (training set and validation set) were entered to calculate the power (1-β err prob), yielding values of 0.977 and 0.967, respectively.

Data analysis was performed using SPSS 29.0 statistical software (SPSS Inc., Chicago, IL, USA). Categorical data were presented as [n (%)]. Continuous variables were tested for normality using the Shapiro-Wilk test. Variables following a normal distribution were expressed as Mean ± SD. Statistical significance was set at P < 0.05. Pearson correlation analysis was used for continuous variables, and Spearman correlation analysis was applied to categorical variables. Univariate and multivariate logistic regression analyses were conducted to identify independent influencing factors, with odds ratios (OR) calculated for each. Receiver operating characteristic (ROC) curves were constructed using CT radiomic features and inflammatory markers to determine the optimal thresholds. Once the predictive model was developed, its performance was further validated through external validation using ROC curves.
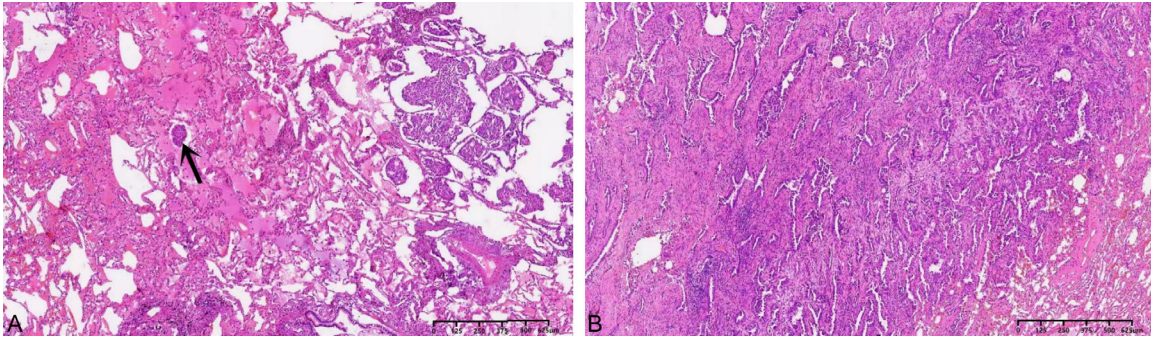
Figure 1. H&E staining. A. A representative STAS case, showing tumor cells within alveolar spaces (20×). B. A representative N-STAS case, showing no tumor cell dissemination (20×).

Results

Comparison of demographic and basic data

Representative hematoxylin and eosin (H&E) stained sections from patients with and without STAS are shown in **Figure 1**. In the STAS group, tumor cells were observed within alveolar spaces, without association to blood vessels or lymphatics, confirming the presence of STAS. In contrast, no such dissemination was noted in the N-STAS group. Baseline characteristics of the N-STAS (n = 141) and STAS (n = 115) groups were compared to evaluate their predictive value for pulmonary adenocarcinoma STAS (**Table 1**). The analysis revealed no significant differences between the two groups in terms of demographics and clinical features, including gender distribution (male/female: 61 [43.26%]/80 [56.74%] in the N-STAS group and 49 [42.61%]/66 [57.39%] in the STAS group; P = 0.916), age (51.21 ± 4.63 years vs. 51.81 ± 4.12 years; P = 0.280), and BMI (22.36 ± 3.19 kg/m^2 vs. 22.27 ± 3.34 kg/m^2; P = 0.826). Habits and medical history, such as smoking status, marital status, clinical symptoms, family history of lung cancer, and prior malignancies, were comparable between the groups (P > 0.05 for all). Tumor location did not differ significantly (P = 0.999). However, statistically significant differences were observed in surgical approaches and mortality rates. The STAS group had a higher prevalence of lobectomy (74.78% vs. 64.54%) and partial resection (15.65% vs. 9.93%) compared to the N-STAS group, while the N-STAS group underwent more segmentectomies (25.53% vs. 9.57%; *P* = 0.003). The STAS group also exhibited a higher mortality rate (16.52% vs. 4.96%; P = 0.002).

No notable differences were observed in comorbidities, such as hypertension, diabetes mellitus, coronary heart disease, and chronic obstructive pulmonary disease (P > 0.05 for all). Overall, surgical approach and mortality were significantly associated with STAS, underscoring their relevance in predicting STAS in pulmonary adenocarcinoma.

Comparison of clinical characteristics

Significant differences in T and N stages were observed between the groups (**Table 2**). The STAS group had a higher proportion of T2 stage tumors (46.96% vs. 30.5%; P = 0.007) and more advanced N stages, particularly N2 (29.57% vs. 14.18%; P = 0.02). Lymphatic invasion was more prevalent in the STAS group (26.96% vs. 12.77%; P = 0.004), as was pleural invasion (33.91% vs. 17.02%; P = 0.002). Recurrence rates were significantly higher in the STAS group (25.22% vs. 10.64%; P = 0.002). No significant differences were observed in perineural invasion, ALK rearrangement, or EGFR status (P > 0.05 for all). These findings suggest that the STAS group was associated with more advanced tumor stages, greater invasiveness, and higher recurrence rates, emphasizing the importance of CT radiomics and inflammatory markers in predicting STAS.

Comparison of CT characteristics

The STAS group had a higher proportion of solid nodules (72.17% vs. 51.06%) and a lower frequency of pure ground-glass opacities (pGGO) and mixed ground-glass opacities (mGGO), showing a significant difference in density (P = 0.003) (**Table 3**). Satellite lesions were more

Table 1. Baseline characteristics

Parameters	N-STAS Group (n = 141)	STAS Group (n = 115)	t/χ²	P
Gender (Male/Female)	61 (43.26%)/80 (56.74%)	49 (42.61%)/66 (57.39%)	0.011	0.916
Age (years)	51.21 ± 4.63	51.81 ± 4.12	1.082	0.28
BMI (kg/m²)	22.36 ± 3.19	22.27 ± 3.34	0.220	0.826
Current Smoking (Yes/no)	60 (42.55%)	51 (44.35%)	0.083	0.773
Marital status (Married/Others)	121 (85.82%)/20 (14.18%)	102 (88.7%)/13 (11.3%)	0.468	0.494
Clinical symptoms (Yes/no)	36 (25.53%)	25 (21.74%)	0.502	0.479
Family history of lung cancer (Yes/no)	7 (4.96%)	5 (4.35%)	0.054	0.816
History of malignancy (Yes/no)	19 (13.48%)	15 (13.04%)	0.01	0.919
Location			0.093	0.999
Left lower lobe	24 (17.02%)	21 (18.26%)		
Left upper lobe	41 (29.08%)	32 (27.83%)		
Right lower lobe	22 (15.6%)	18 (15.65%)		
Right middle lobe	15 (10.64%)	12 (10.43%)		
Right upper lobe	39 (27.66%)	32 (27.83%)		
Surgery			11.416	0.003
Lobectomy	91 (64.54%)	86 (74.78%)		
Partial resection	14 (9.93%)	18 (15.65%)		
Segmentectomy	36 (25.53%)	11 (9.57%)		
Comorbidity				
Hypertension	32 (22.7%)	34 (29.57%)	1.562	0.211
Diabetes mellitus	13 (9.22%)	16 (13.91%)	1.389	0.239
CHD	15 (10.64%)	11 (9.57%)	0.08	0.777
COPD	19 (13.48%)	14 (12.17%)	0.096	0.757
Death (Yes/no)	7 (4.96%)	19 (16.52%)	9.272	0.002

Note: BMI: body mass index; CHD: coronary heart disease; COPD: chronic obstructive pulmonary disease; STAS: spread through air spaces.

Table 2. Compare of clinical characteristics between study groups

Parameters	N-STAS Group (n = 141)	STAS Group (n = 115)	t/χ²	P
T stage			7.292	0.007
T1	98 (69.5%)	61 (53.04%)		
T2	43 (30.5%)	54 (46.96%)		
N stage			9.787	0.02
N0	109 (77.3%)	70 (60.87%)		
N1	9 (6.38%)	9 (7.83%)		
N2	20 (14.18%)	34 (29.57%)		
N3	3 (2.13%)	2 (1.74%)		
Lymphatic invasion (Presence/Absence)	18 (12.77%)/123 (87.23%)	31 (26.96%)/84 (73.04%)	8.241	0.004
Perineural invasion (Presence/Absence)	4 (2.84%)/137 (97.16%)	5 (4.35%)/110 (95.65%)	0.097	0.755
Pleural invasion (Presence/Absence)	24 (17.02%)/117 (82.98%)	39 (33.91%)/76 (66.09%)	9.741	0.002
ALK rearrangement (Presence/Absence)	5 (3.55%)/136 (96.45%)	9 (7.83%)/106 (92.17%)	2.244	0.134
EGFR (Presence/Absence)	81 (57.45%)/60 (42.55%)	62 (53.91%)/53 (46.09%)	0.321	0.571
Recurrence (Yes/no)	15 (10.64%)	29 (25.22%)	9.459	0.002

Note: T stage: Primary Tumor stage; N stage: Nodes stage; ALK rearrangement: Anaplastic Lymphoma Kinase rearrangement; EGFR: Epidermal Growth Factor Receptor; STAS: spread through air spaces.

prevalent in the STAS group (8.7% vs. 1.42%; P = 0.006). Irregular tumor shapes were more common in the STAS group compared to the N-STAS group (22.61% vs. 8.51%; P = 0.002).

Table 3. Compare of CT characteristics between study groups

Parameters	N-STAS Group (n = 141)	STAS Group (n = 115)	χ^2	P
Density			11.974	0.003
pGGO	25 (17.73%)	13 (11.3%)		
mGGO	44 (31.21%)	19 (16.52%)		
Solid	72 (51.06%)	83 (72.17%)		
Satellite lesions (Presence/Absence)	2 (1.42%)/139 (98.58%)	10 (8.70%)/105 (91.3%)	7.508	0.006
Homogeneity (Presence/Absence)	124 (87.94%)/17 (12.06%)	96 (83.48%)/19(16.52%)	1.045	0.307
Shape			9.959	0.002
Round or oval	129 (91.49%)	89 (77.39%)		
Irregular	12 (8.51%)	26 (22.61%)		
Margin			0.116	0.733
Well-defined	68 (48.23%)	53 (46.09%)		
Ill-defined	73 (51.77%)	62 (53.91%)		
Pleural indentation (Presence/Absence)	91 (64.54%)/50 (35.46%)	86 (74.78%)/29 (25.22%)	3.115	0.078
Spiculation (Presence/Absence)	53 (37.59%)/88 (62.41%)	64 (55.65%)/51 (44.35%)	8.328	0.004
Air bronchogram (Presence/Absence)	24 (17.02%)/117 (82.98%)	18 (15.65%)/97 (84.35%)	0.087	0.769
Vascular convergence (Presence/Absence)	56 (39.72%)/85 (60.28%)	67 (58.26%)/48 (41.74%)	8.726	0.003
Vacuole sign (Presence/Absence)	49 (34.75%)/92 (65.25%)	22 (19.13%)/93 (80.87%)	7.712	0.005
Cavity (Presence/Absence)	6 (4.26%)/135 (95.74%)	11 (9.57%)/104 (90.43%)	2.881	0.09

Note: pGGO: pure ground-glass opacity; mGGO: mixed ground-glass opacity; STAS: spread through air spaces.

Spiculation occurred more frequently in the STAS group (55.65% vs. 37.59%; P = 0.004), as did vascular convergence (58.26% vs. 39.72%; P = 0.003). In contrast, the vacuole sign was less common in the STAS group (19.13% vs. 34.75%; P = 0.005). No significant differences were observed in margin definitiveness, pleural indentation, air bronchogram presence, homogeneity, or cavity formation (P > 0.05 for all). These results underscore the distinct CT radiomic features associated with STAS, emphasizing their potential utility in predicting STAS in pulmonary adenocarcinoma.

Comparison of inflammatory markers

The LMR was significantly lower in the STAS group (4.65 ± 1.53) compared to the N-STAS group (5.21 ± 1.36; P = 0.002) (**Figure 2A**). Conversely, the NLR and PLR were higher in the STAS group, with values of 2.24 ± 0.77 and 143.27 ± 41.89, respectively, compared to 1.96 ± 0.67 and 125.71 ± 42.15 in the N-STAS group (P = 0.003 and P = 0.001, respectively) (**Figure 2B**, **2C**). The ALI was significantly lower in the STAS group (41.16 ± 14.28) than in the N-STAS group (47.46 ± 16.35; P = 0.001) (**Figure 2D**), while the SII was higher in the STAS group (603.28 ± 231.44) compared to the N-STAS group (532.13 ± 198.24; P = 0.009) (**Figure 2F**). No significant difference was observed in the PNI between the groups (P =

0.112) (**Figure 2E**). These findings suggest that certain inflammatory markers, such as LMR, NLR, PLR, ALI, and SII, are associated with the presence of STAS in pulmonary adenocarcinoma, indicating their potential role in predicting STAS.

Logistic regression analysis

Among the CT radiomic factors, density (pGGO/mGGO/solid) was significantly associated with STAS, with an odds ratio (OR) of 1.700 (95% CI, 1.200-2.542; P = 0.003) (**Table 4**). The presence of satellite lesions was a strong predictor, with an OR of 6.619 (95% CI, 1.700-43.657; P = 0.016). Irregular shape was inversely related to dissemination (OR, 0.318; 95% CI, 0.148-0.651; P = 0.002), while spiculation (OR, 2.084; 95% CI, 1.266-3.455; P = 0.004) and vascular convergence (OR, 2.119; 95% CI, 1.288-3.513; P = 0.003) were positively correlated. The vacuole sign inversely affected dissemination (OR, 0.444; 95% CI, 0.245-0.785; P = 0.006).

For inflammatory markers, significant predictors included LMR, which showed an inverse association (OR, 0.761; 95% CI, 0.634-0.906; P = 0.003). NLR demonstrated a positive relationship (OR, 1.724; 95% CI, 1.213-2.491; P = 0.003), as did PLR (OR, 1.010; 95% CI, 1.004-1.016; P = 0.001). The ALI had a protective effect (OR, 0.973; 95% CI, 0.957-0.990; P =
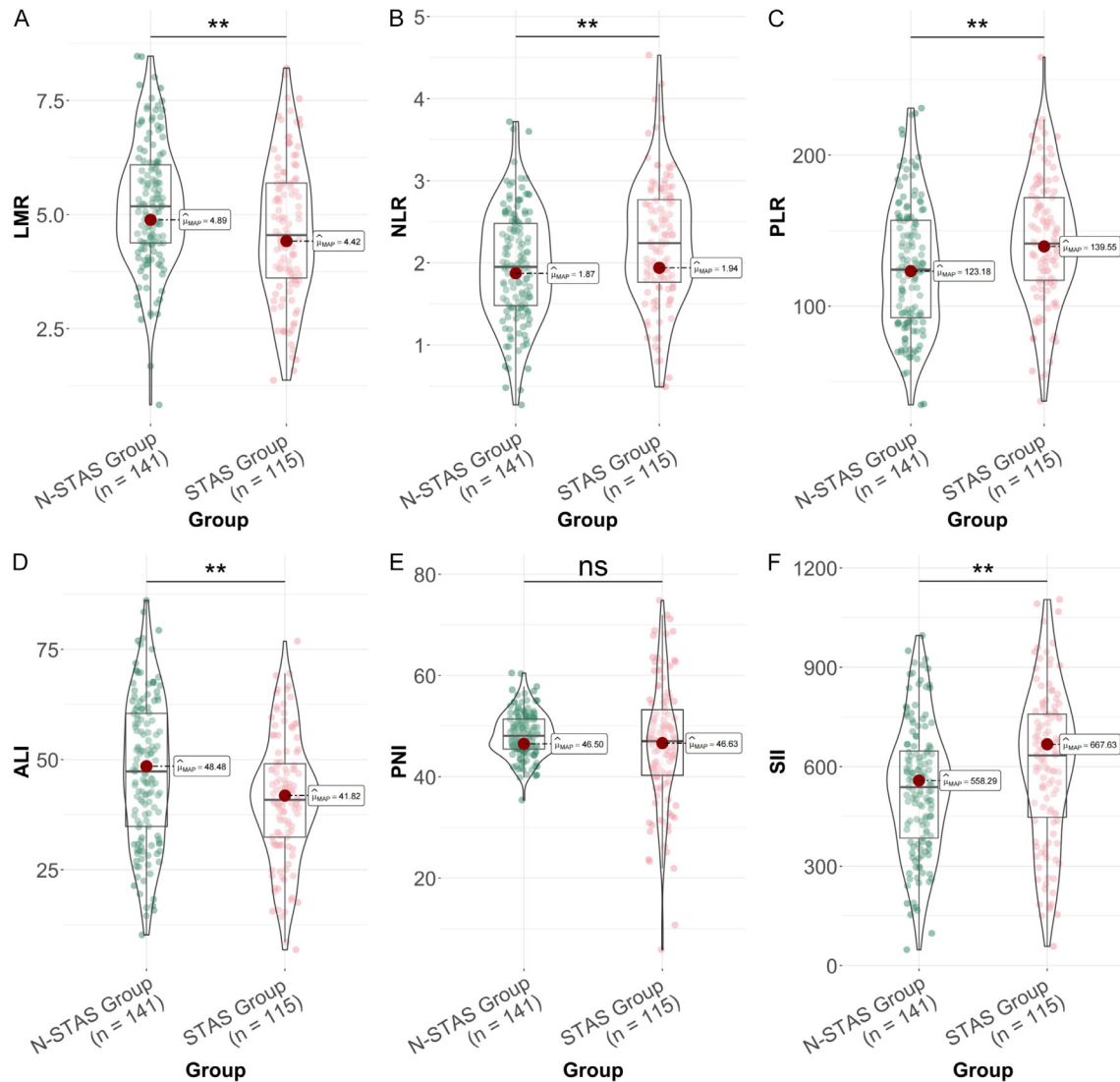
Figure 2. Compare of Inflammatory markers between study groups. A. LMR. B. NLR. C. PLR. D. ALI. E. PNI. F. SII. **: *P* < 0.01, ns: no significant difference. Note: LMR: Lymphocyte-to-Monocyte Ratio; NLR: Neutrophil-to-Lymphocyte Ratio; PLR: Platelet-to-Lymphocyte Ratio; ALI: Advanced Lung Cancer Inflammation Index; PNI: Prognostic Nutritional Index; SII: Systemic Inflammatory Index.

0.002), whereas SII showed a modest association (OR, 1.002; 95% CI, 1.000-1.003; P = 0.010). These results highlight the predictive value of specific CT radiomic features and inflammatory markers for STAS in pulmonary adenocarcinoma.

Multivariate logistic regression analysis

The multivariate logistic regression analysis identified several significant independent risk factors for STAS in pulmonary adenocarcinoma, integrating CT radiomics and inflammatory markers (**Table 5**). Among CT features, density

(pGGO/mGGO/solid) showed a strong association with dissemination, with an OR of 2.279 (95% CI, 1.482-3.505; P < 0.001). The presence of satellite lesions approached significance (OR, 5.508; 95% CI, 0.922-32.913; P = 0.061). An irregular tumor shape was inversely associated with dissemination (OR, 0.330; 95% CI, 0.139-0.781; P = 0.012), whereas spiculation (OR, 2.525; 95% CI, 1.360-4.690; P = 0.003) and vascular convergence (OR, 1.975; 95% CI, 1.077-3.623; P = 0.028) were positively correlated. The vacuole sign demonstrated a protective effect (OR, 0.343; 95% CI, 0.169-0.693; P = 0.003).

Table 4. Univariate logistic regression analysis of CT radiomics and inflammatory markers for STAS in pulmonary adenocarcinoma

Influencing factors	Coefficient	Std. Error	Wald	P	OR	95% CI
Density (pGGO/mGGO/Solid)	0.531	0.182	2.922	0.003	1.700	1.200-2.542
Satellite lesions (Presence/Absence)	1.890	0.785	2.407	0.016	6.619	1.700-43.657
Shape (Round or oval/Irregular)	-1.144	0.375	3.050	0.002	0.318	0.148-0.651
Spiculation (Presence/Absence)	0.734	0.256	2.869	0.004	2.084	1.266-3.455
Vascular convergence (Presence/Absence)	0.751	0.256	2.936	0.003	2.119	1.288-3.513
Vacuole sign (Presence/Absence)	-0.812	0.296	2.744	0.006	0.444	0.245-0.785
LMR	-0.274	0.091	3.014	0.003	0.761	0.634-0.906
NLR	0.545	0.183	2.980	0.003	1.724	1.213-2.491
PLR	0.01	0.003	3.210	0.001	1.010	1.004-1.016
ALI	-0.027	0.009	3.124	0.002	0.973	0.957-0.990
SII	0.002	0.001	2.585	0.010	1.002	1.000-1.003

Note: pGGO: pure ground-glass opacity; mGGO: mixed ground-glass opacity; LMR: Lymphocyte-to-Monocyte Ratio; NLR: Neutrophil-to-Lymphocyte Ratio; PLR: Platelet-to-Lymphocyte Ratio; ALI: Advanced Lung Cancer Inflammation Index; SII: Systemic Inflammatory Index.

Table 5. Multivariate logistic regression analysis of CT radiomics and inflammatory markers for STAS in pulmonary adenocarcinoma

Influencing factors	Coefficient	Std. Error	Wald Stat	P	OR	OR CI Lower	OR CI Upper
Density (pGGO/mGGO/Solid)	0.824	0.220	3.751	< 0.001	2.279	1.482	3.505
Satellite lesions (Presence/Absence)	1.706	0.912	1.871	0.061	5.508	0.922	32.913
Shape (Round or oval/Irregular)	-1.110	0.440	-2.522	0.012	0.330	0.139	0.781
Spiculation (Presence/Absence)	0.926	0.316	2.933	0.003	2.525	1.360	4.690
Vascular convergence (Presence/Absence)	0.681	0.310	2.198	0.028	1.975	1.077	3.623
Vacuole sign (Presence/Absence)	-1.071	0.359	-2.983	0.003	0.343	0.169	0.693
LMR	-0.260	0.107	-2.441	0.015	0.771	0.626	0.950
NLR	0.854	0.233	3.660	< 0.001	2.349	1.487	3.711
PLR	0.004	0.004	1.144	0.253	1.004	0.997	1.012
ALI	-0.036	0.011	-3.328	< 0.001	0.965	0.945	0.985
SII	0.001	0.001	1.950	0.051	1.001	1.000	1.003

Note: pGGO: pure ground-glass opacity; mGGO: mixed ground-glass opacity; LMR: Lymphocyte-to-Monocyte Ratio; NLR: Neutrophil-to-Lymphocyte Ratio; PLR: Platelet-to-Lymphocyte Ratio; ALI: Advanced Lung Cancer Inflammation Index; SII: Systemic Inflammatory Index.

In regard to inflammatory markers, LMR had an inverse relationship with dissemination (OR, 0.771; 95% CI, 0.626-0.950; P = 0.015), while NLR was strongly predictive (OR, 2.349; 95% CI, 1.487-3.711; P < 0.001). Although PLR was not a significant predictor (P = 0.253), ALI was inversely associated with dissemination (OR, 0.965; 95% CI, 0.945-0.985; P < 0.001). The SII showed a marginal association (OR, 1.001; 95% CI, 1.000-1.003; P = 0.051). These findings underscore the pivotal role of specific CT radiomics and inflammatory markers in predicting STAS, potentially aiding in risk stratification and management in pulmonary adenocarcinoma.

ROC curve

We integrated predictive CT radiomic features and inflammatory markers to develop a combined model for predicting STAS in pulmonary adenocarcinoma. This combined model achieved an area under the curve (AUC) of 0.915, indicating high predictive accuracy for STAS (**Figure 3**).

External validation of the predictive model

In the external validation cohort, which compared the N-STAS (n = 121) and STAS (n = 112) groups, baseline characteristics such as sex
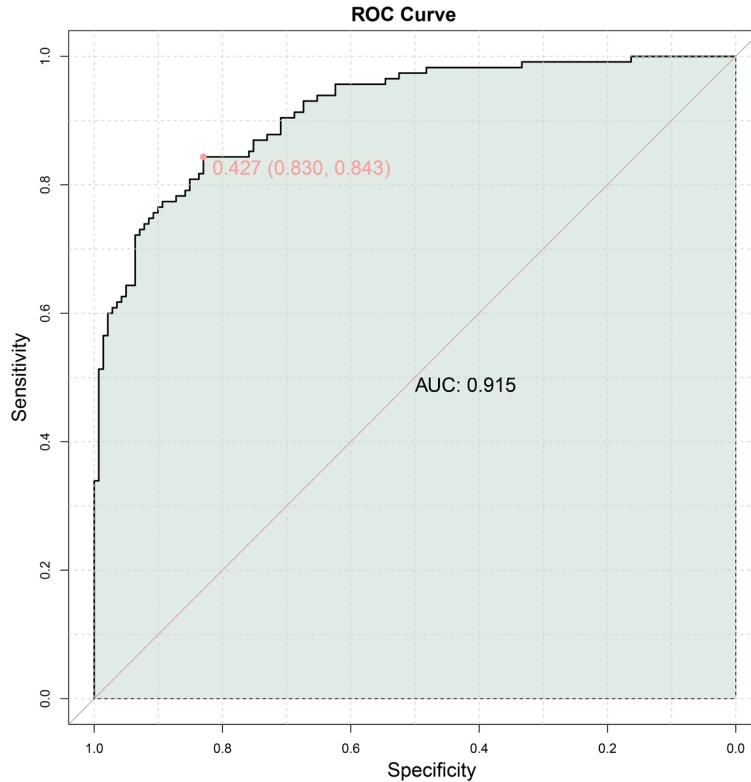
Figure 3. Combined predictive model of CT radiomics and inflammatory markers.

distribution, age, BMI, smoking status, marital status, clinical symptoms, family history of lung cancer, history of malignancy, and tumor location showed no significant differences (P > 0.05) (**Table 6**). The gender distribution and mean ages were comparable between the groups (50.36 ± 5.16 years vs. 50.29 ± 4.98 years; P = 0.909). However, the surgical approach differed significantly between the groups: a higher proportion of patients in the STAS group underwent lobectomy (74.11% vs. 64.46%), while segmentectomy was less frequent (10.71% vs. 25.62%; P = 0.011). Comorbidities, including hypertension, diabetes mellitus, coronary heart disease (CHD), and chronic obstructive pulmonary disease (COPD), were similarly distributed between the groups (P > 0.05 for all). Notably, mortality was significantly higher in the STAS group (16.07% vs. 4.96%; P = 0.005). These findings highlight distinct clinical outcomes related to STAS, with lobectomy being more prevalent in the STAS group and associated with a higher mortality rate.

The analysis revealed that solid nodules were more common in the STAS group (73.21%) com-

pared to the N-STAS group (51.24%), with significant differences in density (P = 0.002) (**Table 7**). Satellite lesions were more frequently observed in the STAS group (12.5% vs. 1.65%; P = 0.001). Tumors in the STAS group were also more likely to have an irregular shape (23.21% vs. 9.09%; P = 0.003). Both spiculation and vascular convergence were more prevalent in the STAS group, at 58.04% and 59.82%, respectively, compared to 37.19% and 39.67% in the N-STAS group (P = 0.001 and P = 0.002, respectively). In contrast, the vacuole sign was less common in the STAS group (18.75% vs. 37.19%; P = 0.002).

Regarding inflammatory markers, the LMR was lower in the STAS group (4.69 ± 1.27) compared to the N-STAS group (5.19 ± 1.13; P = 0.002). The NLR and PLR were higher in the STAS group, at 2.16 ± 0.83 and 131.52 ± 26.74, respectively, compared to 1.86 ± 0.53 and 121.36 ± 21.68 in the N-STAS group (P = 0.001 and P = 0.002, respectively). The ALI was significantly lower in the STAS group (44.39 ± 15.45) compared to the N-STAS group (51.64 ± 17.68; P = 0.001), while the SII was higher (612.69 ± 210.49 vs. 529.67 ± 201.16; P = 0.002).

ROC (external validation)

In the external validation cohort, we integrated the predictive CT radiomic features and inflammatory markers into a combined model for predicting STAS in pulmonary adenocarcinoma. This model achieved an AUC of 0.847, indicating strong predictive accuracy for STAS (**Figure 4**).

Discussion

This study aimed to evaluate the predictive value of CT radiomics and inflammatory markers for STAS in pulmonary adenocarcinoma. CT radiomics, as a non-invasive diagnostic tool,

Table 6. Basic characteristics for external validation

| Parameters	N-STAS Group (n = 121)	STAS Group (n = 112)	t/χ²	P
Gender (Male/Female)	52 (42.98%)/69 (57.02%)	47 (41.96%)/65 (58.04%)	0.024	0.876
Age (years)	50.36 ± 5.16	50.29 ± 4.98	0.114	0.909
BMI (kg/m²)	21.25 ± 2.09	21.41 ± 2.37	0.547	0.585
Current Smoking (Yes/no)	51 (42.15%)/70 (57.85%)	47 (41.96%)/65 (58.04%)	0.001	0.977
Marital status (Married/Others)	104 (85.95%)/17 (14.05%)	99 (88.39%)/13 (11.61%)	0.309	0.578
Clinical symptoms (Yes/no)	30 (24.79%)	24 (21.43%)	0.37	0.543
Family history of lung cancer (Yes/no)	6 (4.96%)	5 (4.46%)	0.032	0.859
History of malignancy (Yes/no)	16 (13.22%)	14 (12.5%)	0.027	0.869
Location			0.188	0.996
Left lower lobe	20 (16.53%)	20 (17.86%)		
Left upper lobe	35 (28.93%)	31 (27.68%)		
Right lower lobe	19 (15.7%)	17 (15.18%)		
Right middle lobe	13 (10.74%)	11 (9.82%)		
Right upper lobe	34 (28.10%)	33 (29.46%)		
Surgery			9.079	0.011
Lobectomy	78 (64.46%)	83 (74.11%)		
Partial resection	12 (9.92%)	17 (15.18%)		
Segmentectomy	31 (25.62%)	12 (10.71%)		
Comorbidity				
Hypertension	27 (22.31%)	33 (29.46%)	1.555	0.212
Diabetes mellitus	11 (9.09%)	15 (13.39%)	1.086	0.297
CHD	13 (10.74%)	11 (9.82%)	0.054	0.817
COPD	16 (13.22%)	14 (12.5%)	0.027	0.869
Death (Yes/no)	6 (4.96%)	18 (16.07%)	7.774	0.005

Note: BMI: body mass index; CHD: coronary heart disease; COPD: chronic obstructive pulmonary disease; STAS: spread through air spaces.

Table 7. Comparison of parameters between study groups

Parameters	N-STAS Group (n = 121)	STAS Group (n = 112)	t/χ²	P
Density			12.046	0.002
pGGO	21 (17.36%)	12 (10.71%)		
mGGO	38 (31.4%)	18 (16.07%)		
Solid	62 (51.24%)	82 (73.21%)		
Satellite lesions (Presence/Absence)	2 (1.65%)/119 (98.35%)	14 (12.5%)/98 (87.5%)	10.701	0.001
Shape			8.685	0.003
Round or oval	110 (90.91%)	86 (76.79%)		
Irregular	11 (9.09%)	26 (23.21%)		
Spiculation (Presence/Absence)	45 (37.19%)/76 (62.81%)	65 (58.04%)/47 (41.96%)	10.141	0.001
Vascular convergence (Presence/Absence)	48 (39.67%)/73 (60.33%)	67 (59.82%)/45 (40.18%)	9.450	0.002
Vacuole sign (Presence/Absence)	45 (37.19%)/76 (62.81%)	21 (18.75%)/91 (81.25%)	9.741	0.002
LMR	5.19 ± 1.13	4.69 ± 1.27	3.145	0.002
NLR	1.86 ± 0.53	2.16 ± 0.83	3.319	0.001
PLR	121.36 ± 21.68	131.52 ± 26.74	3.168	0.002
ALI	51.64 ± 17.68	44.39 ± 15.45	3.322	0.001
SII	529.67 ± 201.16	612.69 ± 210.49	3.078	0.002

Note: pGGO: pure ground-glass opacity; mGGO: mixed ground-glass opacity; LMR: Lymphocyte-to-Monocyte Ratio; NLR: Neutrophil-to-Lymphocyte Ratio; PLR: Platelet-to-Lymphocyte Ratio; ALI: Advanced Lung Cancer Inflammation Index; SII: Systemic Inflammatory Index; STAS: spread through air spaces.
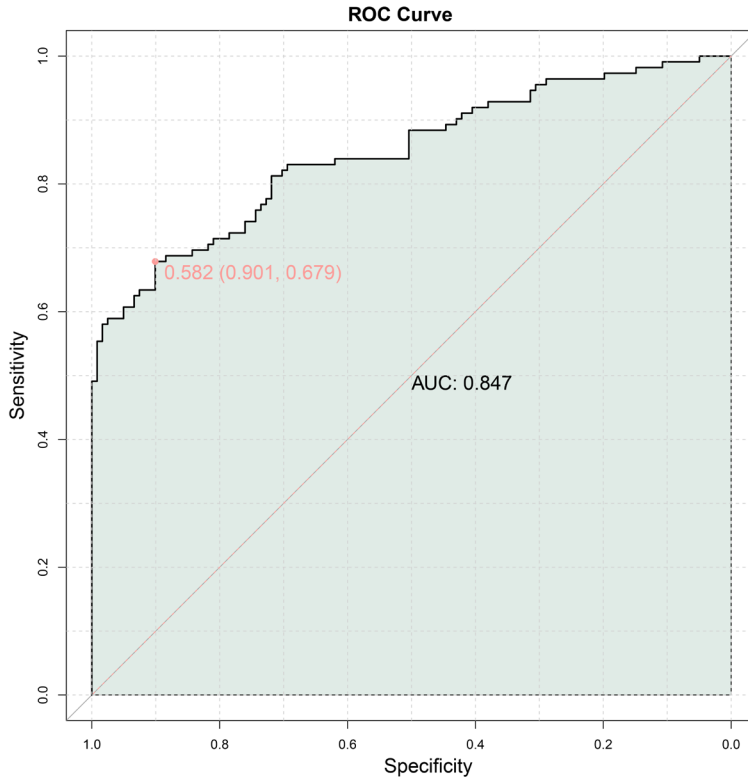
Figure 4. Combined predictive model of CT radiomics and inflammatory markers (external validation).

provides valuable insights into the tumor phenotype by quantifying its imaging characteristics [20-22]. Our results indicate that specific CT features, including density, tumor shape, presence of satellite lesions, spiculation, vascular convergence, and the vacuole sign, play key roles in predicting STAS. Notably, solid nodules were more prevalent among patients with STAS and showed higher density measurements. This could be attributed to increased cellularity and fibrous stroma in solid nodules, which promote tumor invasiveness and subsequent air space seeding. Irregular tumor shape reflects more aggressive tumor behavior, indicating not only localized growth but also a greater potential to invade adjacent structures, facilitating STAS. The increased presence of spiculation and vascular convergence further underscores the invasive phenotype, suggesting interactions with surrounding lung architecture and vasculature, which may favor tumor dispersion.

Our study also revealed a correlation between the presence of STAS and surgical outcomes in pulmonary adenocarcinoma. Patients with STAS were more likely to undergo extensive surgical resections, such as lobectomy and partial resection, compared to those without STAS, who were more frequently treated with segmentectomy. This difference in surgical approaches reflects the increased complexity and aggressiveness of tumors with STAS, which are associated with higher local recurrence rates and poorer prognosis. The higher mortality rate observed in the STAS group further emphasizes the importance of early detection and accurate prediction of STAS to optimize surgical planning and postoperative management.

The presence of satellite lesions in the STAS group highlights a distinct aspect of tumor biology, where multifocal growth patterns may indicate enhanced metastatic capability or tumor budding, both of which are associated with poor clinical outcomes [23, 24]. Interestingly, the vacuole sign, less common in STAS patients, might suggest that its presence indicates less aggressive behavior or a different pathological mechanism that does not favor invasive patterns like STAS. Such distinctions in CT imaging can assist clinicians in stratifying patients at risk for STAS and tailoring treatment protocols accordingly.

Our analysis of inflammatory markers revealed significant associations with STAS, suggesting that systemic inflammation plays a mediating role in oncogenesis and tumor progression. The lower LMR and higher NLR and PLR in the STAS group reflect an overwhelmed immune response and an inflammatory environment that facilitates tumor spread. Pro-inflammatory cytokines, often elevated in such conditions, can enhance tumor cell motility, alter the tumor microenvironment to promote metastasis, and impair anti-tumor immunity. Furthermore, high SII and low ALI indicate chronic inflammation

combined with nutritional deficiencies or cachexia, further weakening host defenses against tumor spread and contributing to worse outcomes [25, 26].

The prognostic relevance of these findings is consistent with the well-established role of inflammation in cancer [27, 28]. Inflammatory markers are not merely passive indicators but active participants in cancer biology, with neutrophils, monocytes, and platelets involved in tumor-promoting processes such as angiogenesis, immune evasion, and dissemination [29]. Neutrophils, through the formation of neutrophil extracellular traps, may create a scaffold that facilitates cancer cell migration and invasion [30, 31], while thrombocytosis (measured by PLR) could enhance circulating tumor cell survival during hematogenous dissemination by providing a protective shield against immune surveillance [14].

However, while PLR was elevated in the STAS group, it did not emerge as a significant predictor in the multivariate logistic regression analysis. This discrepancy warrants further discussion. One possible explanation for the lack of significance of PLR in the multivariate analysis is collinearity between PLR and other inflammatory markers, such as NLR and LMR. Platelets, neutrophils, and lymphocytes are all part of the systemic inflammatory response, and their interactions can be complex. In our study, the strong correlations between these markers may have introduced redundancy in the multivariate model, reducing the independent predictive value of PLR. Additionally, the biological mechanisms underlying PLR may differ from those of NLR and LMR. While NLR and LMR primarily reflect the balance between pro-inflammatory and anti-inflammatory cells, PLR captures the interaction between platelets (involved in coagulation and tumor promotion) and lymphocytes. The role of platelets in cancer progression is multifaceted, and their impact on prognosis may be context-dependent, influenced by factors such as thrombosis, angiogenesis, and immune modulation.

Another factor to consider is the heterogeneity of the patient population. Pulmonary adenocarcinoma is a heterogeneous disease with varying molecular subtypes and clinical presentations. The influence of PLR on prognosis may differ across subgroups, and its predictive power might be diluted in a mixed cohort. Future studies with larger sample sizes and detailed subgroup analyses could help clarify the role of PLR in specific patient populations.

Furthermore, the association between these biomarkers and STAS underscores the complex interplay between systemic inflammation and localized tumor dynamics. This relationship highlights the potential for therapeutic intervention, where anti-inflammatory strategies or modulation of specific inflammatory pathways could complement existing oncological treatments, reducing the risk of STAS and improving patient prognosis.

It is noteworthy that the external validation of our predictive model demonstrated strong alignment with our initial findings, reinforcing the robustness and generalizability of CT radiomics combined with inflammatory markers as predictive tools for STAS. This external validation enhances the clinical applicability of our findings, suggesting that institutions with diverse patient demographics can adopt these predictive markers to efficiently stratify risk among pulmonary adenocarcinoma patients.

The predictive model developed in this study holds significant promise for clinical application. By integrating CT radiomics and inflammatory markers, clinicians can make more informed decisions regarding surgical planning and postoperative management. For example, patients identified as high-risk for STAS may benefit from more aggressive surgical interventions or adjuvant treatments, while those at low risk may avoid unnecessary procedures. Additionally, this model can be used to monitor disease progression and evaluate treatment efficacy over time, providing valuable insights into patient management. The ultimate goal is to translate these findings into clinical guidelines that can improve patient care and outcomes.

However, this study, while providing valuable insights, acknowledges several limitations. Firstly, its retrospective design may introduce selection bias, potentially influencing the generalizability of the findings. Additionally, although the sample size is sufficient for preliminary analysis, it may limit statistical power and the ability to detect subtle associations. Furthermore, the reliance on CT imaging and sys-

temic inflammatory markers, without incorporating molecular or genetic data, may result in an incomplete understanding of the underlying biological mechanisms. Lastly, variations in imaging techniques and analysis across institutions could impact the external validation of the predictive model. Future prospective studies with larger, more diverse cohorts and integrated multi-omics approaches are needed to validate and expand these findings.

In conclusion, the integration of CT radiomics and systemic inflammatory markers offers a promising predictive strategy for STAS in pulmonary adenocarcinoma. These findings underscore the importance of a multi-modal approach in oncology, one that incorporates detailed imaging phenotypes and systemic physiological markers to refine patient prognostication and personalize treatment strategies. Ultimately, the insights gained from this study highlight both the tangible clinical benefits and the promising research directions for understanding the dissemination of pulmonary adenocarcinoma through intricate biological mechanisms.

Disclosure of conflict of interest

None.

Address correspondence to: Mingqing Kou, Department of Radiology, Shaanxi Provincial People's Hospital, No. 256 Youyi West Road, Xi'an 710068, Shaanxi, China. E-mail: kmq9876@126.com

References

[1] Succony L, Rassl DM, Barker AP, McCaughan FM and Rintoul RC. Adenocarcinoma spectrum lesions of the lung: detection, pathology and treatment strategies. Cancer Treat Rev 2021; 99: 102237.

[2] Tan Y, Huang YH, Xue JW, Zhang R, Liu R, Wang Y and Feng ZB. Clinicopathological features and prognostic significance of pulmonary adenocarcinoma with signet ring cell components: meta-analysis and SEER analysis. Clin Exp Med 2023; 23: 4341-4354.

[3] Chen X, Zhou H, Wu M, Xu M, Li T, Wang J, Sun X, Tsutani Y and Xie M. Prognostic impact of spread through air spaces in patients with ≤ 2 cm stage IA lung adenocarcinoma. J Thorac Dis 2024; 16: 2432-2442.

[4] Fan L and He P. Research progress on spread through air spaces of lung cancer. Zhongguo Fei Ai Za Zhi 2022; 25: 54-60.

[5] Almeida GL, Pinto BM, Pinto VM, Tregnago AC, Almeida RF and Pinto Filho DR. Tumor spread through air spaces in lung cancer: prospective analysis of the accuracy of intraoperative frozen section examination. J Bras Pneumol 2024; 50: e20240165.

[6] Ou DX, Lu CW, Chen LW, Lee WY, Hu HW, Chuang JH, Lin MW, Chen KY, Chiu LY, Chen JS, Chen CM and Hsieh MS. Deep learning analysis for predicting tumor spread through air space in early-stage lung adenocarcinoma pathology images. Cancers (Basel) 2024; 16: 2132.

[7] Miranda J, Horvat N, Araujo-Filho JAB, Albuquerque KS, Charbel C, Trindade BMC, Cardoso DL, de Padua Gomes de Farias L, Chakraborty J and Nomura CH. The role of radiomics in rectal cancer. J Gastrointest Cancer 2023; 54: 1158-1180.

[8] Xia T, Zhao B, Li B, Lei Y, Song Y, Wang Y, Tang T and Ju S. MRI-based radiomics and deep learning in biological characteristics and prognosis of hepatocellular carcinoma: opportunities and challenges. J Magn Reson Imaging 2024; 59: 767-783.

[9] Russo L, Charles-Davies D, Bottazzi S, Sala E and Boldrini L. Radiomics for clinical decision support in radiation oncology. Clin Oncol (R Coll Radiol) 2024; 36: e269-e281.

[10] Sohn JH and Fields BKK. Radiomics and deep learning to predict pulmonary nodule metastasis at CT. Radiology 2024; 311: e233356.

[11] Kennel KB, Bozlar M, De Valk AF and Greten FR. Cancer-associated fibroblasts in inflammation and antitumor immunity. Clin Cancer Res 2023; 29: 1009-1016.

[12] Wan L, Wu C, Luo S and Xie X. Prognostic value of lymphocyte-to-monocyte ratio (LMR) in cancer patients undergoing immune checkpoint inhibitors. Dis Markers 2022; 2022: 3610038.

[13] Cupp MA, Cariolou M, Tzoulaki I, Aune D, Evangelou E and Berlanga-Taylor AJ. Neutrophil to lymphocyte ratio and cancer prognosis: an umbrella review of systematic reviews and meta-analyses of observational studies. BMC Med 2020; 18: 360.

[14] Chen W, Xin S and Xu B. Value research of NLR, PLR, and RDW in prognostic assessment of patients with colorectal cancer. J Healthc Eng 2022; 2022: 7971415.

[15] Song M, Zhang Q, Song C, Liu T, Zhang X, Ruan G, Tang M, Xie H, Zhang H, Ge Y, Li X, Zhang K, Yang M, Li Q, Liu X, Lin S, Xu Y, Xu H, Wang K, Li W and Shi H. The advanced lung cancer inflammation index is the optimal inflammatory biomarker of overall survival in patients with lung cancer. J Cachexia Sarcopenia Muscle 2022; 13: 2504-2514.

[16] Zhang L, Ma W, Qiu Z, Kuang T, Wang K, Hu B and Wang W. Prognostic nutritional index as a prognostic biomarker for gastrointestinal cancer patients treated with immune checkpoint inhibitors. Front Immunol 2023; 14: 1219929.

[17] Tian BW, Yang YF, Yang CC, Yan LJ, Ding ZN, Liu H, Xue JS, Dong ZR, Chen ZQ, Hong JG, Wang DX, Han CL, Mao XC and Li T. Systemic immune-inflammation index predicts prognosis of cancer immunotherapy: systemic review and meta-analysis. Immunotherapy 2022; 14: 1481-1496.

[18] Zhang C, Mei Z, Pei J, Abe M, Zeng X, Huang Q, Nishiyama K, Akimoto N, Haruki K, Nan H, Meyerhardt JA, Zhang R, Li X, Ogino S and Ugai T. A modified tumor-node-metastasis classification for primary operable colorectal cancer. JNCI Cancer Spectr 2020; 5: pkaa093.

[19] Nicholson AG, Tsao MS, Beasley MB, Borczuk AC, Brambilla E, Cooper WA, Dacic S, Jain D, Kerr KM, Lantuejoul S, Noguchi M, Papotti M, Rekhtman N, Scagliotti G, van Schil P, Sholl L, Yatabe Y, Yoshida A and Travis WD. The 2021 WHO classification of lung tumors: impact of advances since 2015. J Thorac Oncol 2022; 17: 362-387.

[20] Ge G and Zhang J. Feature selection methods and predictive models in CT lung cancer radiomics. J Appl Clin Med Phys 2023; 24: e13869.

[21] Liu C, Zhao W, Xie J, Lin H, Hu X, Li C, Shang Y, Wang Y, Jiang Y, Ding M, Peng M, Xu T, Hu A, Huang Y, Gao Y, Liu X, Liu J and Ma F. Development and validation of a radiomics-based nomogram for predicting a major pathological response to neoadjuvant immunochemotherapy for patients with potentially resectable non-small cell lung cancer. Front Immunol 2023; 14: 1115291.

[22] Tong H, Sun J, Fang J, Zhang M, Liu H, Xia R, Zhou W, Liu K and Chen X. A machine learning model based on PET/CT radiomics and clinical characteristics predicts tumor immune profiles in non-small cell lung cancer: a retrospective multicohort study. Front Immunol 2022; 13: 859323.

[23] Ozturk A, Ilgun S, Ucuncu M, Gachayev F, Ordu C, Alco G, Elbuken F, Erdogan Z, Duymaz T, Aktepe F, Soybir G and Ozmen V. The effect of multifocal and multicentric tumours on local recurrence and survival outcomes in breast cancer. J BUON 2021; 26: 196-203.

[24] Werner R, Steinmann N, Decaluwe H, Date H, De Ruysscher D and Opitz I. Complex situations in lung cancer: multifocal disease, oligoprogression and oligorecurrence. Eur Respir Rev 2024; 33: 230200.

[25] He K, Si L, Pan X, Sun L, Wang Y, Lu J and Wang X. Preoperative systemic immune-inflammation index (SII) as a superior predictor of long-term survival outcome in patients with stage I-II gastric cancer after radical surgery. Front Oncol 2022; 12: 829689.

[26] Ruan GT, Ge YZ, Xie HL, Hu CL, Zhang Q, Zhang X, Tang M, Song MM, Zhang XW, Liu T, Li XR, Zhang KP, Yang M, Li QQ, Chen YB, Yu KY, Braga M, Cong MH, Wang KH, Barazzoni R and Shi HP. Association between systemic inflammation and malnutrition with survival in patients with cancer sarcopenia-a prospective multicenter study. Front Nutr 2022; 8: 811288.

[27] Shah SC and Itzkowitz SH. Colorectal cancer in inflammatory bowel disease: mechanisms and management. Gastroenterology 2022; 162: 715-730, e713.

[28] Silva AL, Faria M and Matos P. Inflammatory microenvironment modulation of alternative splicing in cancer: a way to adapt. Adv Exp Med Biol 2020; 1219: 243-258.

[29] Peixoto RD, Ferreira AR, Cleary JM, Fogacci JP, Vasconcelos JP and Jácome AA. Risk of cancer in inflammatory bowel disease and pitfalls in oncologic therapy. J Gastrointest Cancer 2023; 54: 357-367.

[30] Hedrick CC and Malanchi I. Neutrophils in cancer: heterogeneous and multifaceted. Nat Rev Immunol 2022; 22: 173-187.

[31] Ng MSF, Tan L, Wang Q, Mackay CR and Ng LG. Neutrophils in cancer-unresolved questions. Sci China Life Sci 2021; 64: 1829-1841.